



This is a repository copy of *A cortex-specific PBP contributes to cephalosporin resistance in Clostridium difficile*.

White Rose Research Online URL for this paper:
<http://eprints.whiterose.ac.uk/149079/>

Version: Submitted Version

Article:

Alabdali, Y.A.J., Oatley, P., Kirk, J.A. et al. (1 more author) (Submitted: 2019) A cortex-specific PBP contributes to cephalosporin resistance in *Clostridium difficile*. bioRxiv. (Submitted)

<https://doi.org/10.1101/715458>

© 2019 The Author(s). This paper is made available under a CC-BY-NC 4.0 International license (<http://creativecommons.org/licenses/by-nc/4.0/>).

Reuse

This article is distributed under the terms of the Creative Commons Attribution-NonCommercial (CC BY-NC) licence. This licence allows you to remix, tweak, and build upon this work non-commercially, and any new works must also acknowledge the authors and be non-commercial. You don't have to license any derivative works on the same terms. More information and the full terms of the licence here:
<https://creativecommons.org/licenses/>

Takedown

If you consider content in White Rose Research Online to be in breach of UK law, please notify us by emailing eprints@whiterose.ac.uk including the URL of the record and the reason for the withdrawal request.



eprints@whiterose.ac.uk
<https://eprints.whiterose.ac.uk/>

1 **A cortex-specific PBP contributes to cephalosporin resistance in**
2 ***Clostridium difficile***

3 **Yasir Adil Jabbar Alabdali^{1,2}, Peter Oatley¹, Joseph A. Kirk¹, Robert P. Fagan^{1*}**

4 ¹Florey Institute, Department of Molecular Biology and Biotechnology, University of
5 Sheffield, UK

6 ²Current address: Department of Biology, College of Science, Al Muthanna University, Iraq

7

8

9 * **Correspondence:**

10 Corresponding Author

11 r.fagan@sheffield.ac.uk

12 **Keywords: *Clostridium difficile*, sporulation, SpoVD, peptidoglycan, penicillin binding**
13 **protein, antimicrobial resistance**

14

15

16

17 Original research article

18 Text word count: 6,603, 4 figures and 3 tables.

19

20

21 **Abstract**

22 Sporulation is a complex cell differentiation programme shared by many members of the
23 Firmicutes, the end result of which is a highly resistant, metabolically inert spore that can
24 survive harsh environmental insults. *Clostridium difficile* spores are essential for transmission
25 of disease and are also required for recurrent infection. However, the molecular basis of
26 sporulation is poorly understood, despite parallels with the well-studied *Bacillus subtilis*
27 system. The spore envelope consists of multiple protective layers, one which is a specialised
28 layer of peptidoglycan, called the cortex, that is essential for the resistant properties of the
29 spore. We have identified and characterised a penicillin binding protein (PBP) that is required
30 for cortex synthesis in *C. difficile*. Surprisingly this PBP was also found to contribute to
31 cephalosporin resistance, indicating an additional role in the synthesis of vegetative cell wall.
32 This is the first description of a cortex-specific PBP in *C. difficile* and begins the process of
33 unravelling cortex biogenesis in this important pathogen.

34

35 Introduction

36 *C. difficile* is the most common cause of nosocomial antibiotic-associated diarrhea, with an
37 estimated 453,000 infections and 29,300 deaths per year in the USA alone (Lessa et al., 2015).
38 *C. difficile* infection (CDI) requires prior disruption to the gut microbiota, most commonly due
39 to an administered antibiotic (Smits et al., 2016). As current treatments largely rely on
40 antibiotic therapy, with further consequent damage to the microbiota, recurrent disease is
41 common and is associated with worse patient prognosis (Rupnik et al., 2009). In recent years
42 there have been dramatic changes in *C. difficile* epidemiology, in particular due to the
43 emergence of the epidemic ribotype 027 lineage, a previously rare ribotype that was
44 responsible for a series of large hospital outbreaks in North America in the early years of this
45 century before spreading worldwide (He et al., 2013).

46 The spore is an absolute requirement for transmission of disease (Deakin et al., 2012), it allows
47 the organism to transit the lethal aerobic environment while also providing significant
48 resistance to desiccation, heat and common disinfectants (Dyer et al., 2019). As a result, the
49 spores shed by an infected individual can survive in the environment for an extended period of
50 time, a particular problem in hospital environments where large numbers of susceptible
51 individuals are housed in close proximity. The process of sporulation is still relatively poorly
52 understood, despite significant advances in recent years (Zhu et al., 2018). We have previously
53 used high-density transposon mutagenesis and TraDIS to identify a subset of *C. difficile* genes
54 required for formation of mature heat-resistance spores (Dembek et al., 2015). In total,
55 transposon insertions in 798 genes were found to significantly impact sporulation, many with
56 no clear homology to previously characterised proteins. Very few of these 798 genes have been
57 studied in *C. difficile* but many have homologues in the well-studied *Bacillus subtilis*
58 sporulation pathway. However, despite the clear parallels between sporulation in *B. subtilis*
59 and *C. difficile*, there are enough critical differences to greatly reduce the value of assumptions
60 based on homology (Paredes et al., 2005; Underwood et al., 2009; Fimlaid et al., 2013). The
61 response regulator Spo0A is the master regulator of sporulation, phosphorylation of which sets
62 in motion a complex asymmetric cell differentiation programme involving the sequential
63 activation of a series of dedicated sigma factors that are in turn responsible for the expression
64 of the individual regulons required for correct spore morphogenesis (Paredes-Sabja et al.,
65 2014). The result is the complex multi-layered spore structure that lends robustness to
66 environmental insult. The spore consists of a dehydrated core surrounded by a membrane and
67 peptidoglycan cell wall (primordial wall) derived from the mother cell envelope. Around this
68 is a thick peptidoglycan cortex, synthesised during spore maturation, and a second membrane,

69 formed as a result of engulfment of the prespore by the mother cell. The outer surface consists
70 of multiple layers of highly crosslinked proteins. The order and timing of synthesis of each of
71 these layers is critical and disruption to any of the steps typically results in the formation of
72 defective spores that lack full resistance properties (Fimlaid et al., 2013).

73 In *B. subtilis* the peptidoglycan of the primordial wall and cortex differ in structure allowing
74 differentiation by the cortex lytic hydrolases during germination (Gilmore et al., 2004). The
75 primordial cell wall consists of typical alternating β -1 \rightarrow 4-linked N-acetyl glucosamine and N-
76 acetyl muramic acid residues, crosslinked by 4-3 linked peptide stems attached to the muramic
77 acid moieties, while in the cortex peptidoglycan every second N-acetyl muramic acid is
78 modified to muramic- δ -lactam, resulting in fewer stem peptides, fewer crosslinks and a more
79 flexible overall structure (Meador-Parton and Popham, 2000). The class B penicillin binding
80 protein (PBP) SpoVD is critical for synthesis of *B. subtilis* cortex (Daniel et al., 1994). During
81 sporulation SpoVD is expressed in the mother cell where it interacts with the SEDS protein
82 SpoVE to enable localisation to the asymmetric division septum (Fay et al., 2010). An N-
83 terminal transmembrane alpha helix anchors the protein in the membrane, placing the majority
84 of the protein in the inter-membrane space where the cortex is ultimately synthesised (Sidarta
85 et al., 2018). The protein consists of a PBP dimerization domain, followed by a transpeptidase
86 domain and a penicillin-binding protein and serine/threonine kinase associated (PASTA)
87 domain, the last of which is dispensable for cortex formation (Bukowska-Faniband and
88 Hederstedt, 2015).

89 *C. difficile* vegetative cell peptidoglycan is superficially similar to that of *B. subtilis*, albeit with
90 a preponderance of 3-3 cross-linking as a result of L,D-transpeptidase activity (Peltier et al.,
91 2011). The structure of the *C. difficile* cortex peptidoglycan has not been determined, although
92 it is assumed to contain muramic- δ -lactam, and the enzymes required for cortex synthesis have
93 not yet been characterised. Here we set out to identify and characterise the major *C. difficile*
94 cortex PBP.

95

96 **Methods**

97 **Bacterial strains and growth conditions**

98 All bacterial strains, plasmids and oligonucleotides used in this study are described in Table 1.
99 *E. coli* strains were routinely grown in LB broth and on LB agar, while *C. difficile* strains were
100 grown in TY broth (Dupuy and Sonenshein, 1998) and on brain heart infusion agar. Cultures
101 were supplemented with chloramphenicol (15 µg/ml), thiamphenicol (15 µg/ml) or cycloserine
102 (250 µg/ml) as appropriate.

103

104 **Molecular biology methods**

105 Routine molecular biology techniques were performed according to the manufacturers
106 protocols except where otherwise stated. PCR using Phusion High-Fidelity DNA Polymerase,
107 plasmid isolation and purification of DNA fragments were performed using kits and reagents
108 supplied by Thermo Fisher Scientific according to the manufacturer's instructions. Restriction
109 digestion, ligation and Gibson assembly were performed with enzymes supplied by New
110 England Biolabs. Competent *E. coli* were transformed using standard methods and plasmid
111 DNA was transferred to *C. difficile* as described previously (Kirk and Fagan, 2016). *C. difficile*
112 mutants were constructed by homologous recombination as described previously (Cartman et
113 al., 2012; Ng et al., 2013). Mutants were confirmed by PCR and Southern blotting using the
114 Amersham ECL Direct Labelling and Detection System kit (GE) according to the
115 manufacturer's instructions. A 230 bp probe to the region immediately upstream of *spoVD* was
116 generated by PCD using primer pair RF461/RF462.

117

118 **Plasmid construction**

119 pJAK032: pRPF150 was modified by inverse PCR using primer pair NF1957/NF1958 to
120 introduce an XhoI site between the Strep Tag II and SecA2 coding sequences, yielding
121 pJAK012. The Strep Tag II coding sequence was then excised using SacI and XhoI and
122 replaced with a synthetic DNA fragment (IDT gBlock) consisting of a codon-optimized *clip*
123 gene, modified by PCR with primer pair RF226/RF227 to add appropriate SacI and XhoI sites.
124 pYAA024: Homology arms upstream and downstream of *spoVD* were amplified by PCR using
125 oligonucleotide pairs RF68/RF139 and RF69/RF187. The resulting PCR products were joined
126 together in a SOEing PCR reaction and cloned between the BamHI and SacI sites in pMTL-
127 YN4.

128 pYAA027: *spoVD* expression appears to be driven from a promoter upstream of R20291_2545.
129 In order to ensure complementation at wild type levels a fragment comprising 282 bp upstream

130 of R20291_2545, R20291_2545 itself and *spoVD* was amplified by PCR using primer pair
131 RF324/RF325 and cloned between BamHI and SacI sites in pMTL-YN2C.
132 pYAA031: *secA2* in pJAK032 was replaced by *spoVD*. *spoVD* was amplified by PCR using
133 primer pair RF374/RF375, digested with BamHI and XhoI and ligated to pJAK032 backbone
134 cut with the same enzymes.
135 pYAA047: 1,200 bp upstream of *spoVD*, the *snap* tag gene from pFT46 and the first 1,200 bp
136 of *spoVD* were amplified by PCR using primer pairs, RF528/RF529, RF530/RF531 and
137 RF532/RF533 respectively. pMTL-SC7215 was linearized by PCR using primer pair
138 RF20/RF311. The four DNA fragments were then joined in a Gibson assembly reaction.
139 pYAA048-050: The coding sequence of the SpoVD PBP dimerization domain (pYAA048;
140 primers RF582/RF583), PASTA domain (pYAA049; primers RF584/RF585), or
141 transpeptidase domain (pYAA050; primers RF586/RF587) were deleted by modification of
142 pYAA031 by inverse PCR and subsequent recircularization by ligation.
143 pYAA051: pYAA048 was further modified to delete the coding sequence of the PASTA
144 domain by inverse PCR with primers RF584/RF585.

145

146 **Sporulation efficiency analysis**

147 Overnight cultures of *C. difficile* R20291 were diluted in BHI broth to an OD_{600nm} of 0.01,
148 incubated for 8 h at 37°C, diluted to an OD_{600nm} of 0.0001 and finally incubated overnight. This
149 allowed us to obtain cultures in stationary phase with no detectable spores (T=0). This culture
150 was then incubated for 5 days with vegetative cells and spores enumerated daily. For total
151 viable counts, 10-fold serial dilutions were spotted onto BHIS agar supplemented with 0.1%
152 sodium taurocholate. For total spore counts, the same process was carried out following a 30
153 min incubation at 65°C. Colonies were counted after 24 h incubation at 37°C and the assay was
154 completed in biological triplicates. Formation of phase bright spores was also followed by
155 phase-contrast microscopy at each time point. Samples fixed in 3.7% paraformaldehyde were
156 imaged using a Nikon Eclipse Ti microscope and analysed using Fiji (Schindelin et al., 2012).

157

158 **Microscopy**

159 Bacterial samples were harvested by centrifugation, washed once with PBS and fixed in 4%
160 paraformaldehyde. For phase contrast microscopy, samples were mounted in 80% glycerol and
161 imaged using a Nikon Ti Eclipse inverted microscope. Samples for transmission electron
162 microscopy were fixed as above before additional fixation in 3% glutaraldehyde, 0.1 M
163 cacodylate buffer. Fixed samples were then treated with 1% OsO₄, dehydrated in ethanol and

164 embedded in araldite resin. Embedded samples were sectioned at 85 nm on a Leica UC6
165 ultramicrotome, transferred onto coated copper grids, further stained with uranyl acetate and
166 lead citrate and visualized using a FEI Tecnai BioTWIN TEM at 80 kV fitted with a Gatan
167 MS600CW camera.

168 For fluorescence confocal microscopy, bacteria were grown in TY broth containing 500 nM
169 HADA (Kuru et al., 2015), labelled with 250 nM SNAP-Cell TMR-Star (New England
170 Biolabs) and grown under anaerobic conditions for a further 60 min. Following labelling, cells
171 were harvested at 8,000 x g for 2 min at 4°C and washed twice in 1 ml ice cold PBS. Cells
172 were resuspended in PBS and fixed in a 4% paraformaldehyde at room temperature for 30 min
173 with agitation. Cells were washed three times in 1 ml ice cold PBS, immobilized by drying to
174 a coverslip and mounted in SlowFade Diamond (Thermo Fisher Scientific). Images were
175 captured using a Zeiss AiryScan confocal microscope.

176

177 **Antibiotic minimum inhibitory concentrations (MICs)**

178 MICs were determined using the agar dilution method based on the Clinical and Laboratory
179 Standards Institute guidelines (Clinical and Laboratory Standards Institute, 2012). Briefly, agar
180 plates were prepared with a range of concentrations of each antibiotic (2 µg/ml to 1024 µg/ml)
181 using BHI supplemented with defibrinated horse blood (Oxoid) or Brazier's CCEY agar plates
182 (Bioconnections) supplemented with egg yolk emulsion (Oxoid) and defibrinated horse blood
183 (Oxoid). The plates were dried at room temperature for 2 h and then pre-reduced in the
184 anaerobic cabinet for 2 h. 100 µl of each *C. difficile* strain at an OD_{600nm} of 0.5 was spread onto
185 the plates. The plates were incubated for 48 h in the anaerobic cabinet at 37°C) and MICs were
186 determined by reading the lowest antibiotic concentration on which the bacteria did not grow.

187

188 **Results**

189 ***C. difficile* produces a SpoVD homologue that is required for sporulation**

190 The *C. difficile* R20291 genome encodes 10 putative penicillin binding proteins (PBPs) (Table
191 2) and one predicted monofunctional transglycosylase (CDR20291_2283). In our previous
192 transposon mutagenesis study only two of these, CDR20291_0712 and 0985, were identified
193 as essential for growth *in vitro* (Dembek et al., 2015). However, five of the PBPs were required
194 for formation of heat-resistant spores, including two with homology to the *B. subtilis* cortex
195 specific PBP SpoVD, CDR20291_1067 and 2544. Of these only CDR20291_2544 has the C
196 terminal PASTA domain that is characteristic of the *B. subtilis* sporulation-specific PBPs
197 (Bukowska-Faniband and Hederstedt, 2015). CDR20291_2544 (SpoVDC_d) shares 40.1%
198 amino acid identity with *B. subtilis* SpoVD and has the same predicted overall organisation,
199 with an N terminal predicted transmembrane helix, followed by a PBP dimerization domain
200 (PF03717), a transpeptidase domain (PF00905) and the C. terminal PASTA domain
201 (PF03793). *spoVD* is located immediately downstream of CDR20291_2545 (Fig. 2A),
202 encoding a protein with weak homology to *B. subtilis* FtsL (18.8% amino acid identity).
203 Despite the weak similarity, the *C. difficile* and *B. subtilis* proteins are very similar in size (115
204 and 117 amino acids respectively), have a similar PI (9.57 and 9.63 respectively) and both have
205 a high proportion of lysine residues (22.6% and 14.5% respectively). CDR20291_2545 and
206 *spoVD* appear to be in an operon, with the promoter upstream of CDR20291_2545. In our
207 earlier TraDIS screen, CDR20291_2545 was also found to be required for sporulation,
208 although this may have been due to polar effects on *spoVD*.

209

210 To confirm a role in sporulation, we constructed a clean *spoVD* deletion by homologous
211 recombination and then complemented this mutant by integrating the CDR20291_2545-*spoVD*
212 cassette under the control of the native promoter into the chromosome between the *pyrE* and
213 R20291_0189 genes (referred to here as R20291Δ*spoVD pyrE::spoVD*; Fig. 1A and B). We
214 then analysed the ability of each strain to form heat-resistant spores. In our assay, a stationary
215 phase culture of wild type R20291 gradually accumulated spores, accounting for 81% of the
216 viable counts after 3 days (Fig 1C). In the same assay R20291Δ*spoVD* formed no detectable
217 spores, even after 5 days of incubation (Fig 1D). Complementation completely restored
218 sporulation to wild type levels (Fig 1E). Examination by phase contrast microscopy confirmed
219 the presence of abundant mature phase bright spores in 5 day old cultures of wild type R20291
220 and the complemented strain R20291Δ*spoVD pyrE::spoVD* (Fig. 2A). In contrast no phase

221 bright objects were observed in cultures of R20291 Δ *spoVD*. When visualised at higher
222 magnification using TEM of thin sections, no morphologically normal spores were observed
223 in cultures of R20291 Δ *spoVD* (Fig. 2B). Membrane-bound prespores were present, but these
224 structures were irregular in shape and crucially lacked the cortex and protein coat layers seen
225 in R20291 and the complemented strain developing spores. SpoVD is predicted to consist of 3
226 domains: a PBP dimerization domain, a transpeptidase domain and a PASTA domain (Fig.
227 3A). To identify which of these were required for viable spore formation, *clip-spoVD* was
228 placed under the control of a constitutive promoter (P_{cwp2}) in a *C. difficile* expression vector
229 and a panel of mutants, lacking one or more of these domains, were constructed (Table 1).
230 These plasmids were all transferred into R20291 Δ *spoVD* and the ability of the expressed
231 SpoVD variant to restore sporulation was evaluated. Only proteins including both the
232 dimerization and transpeptidase domains (SpoVD(DT) or full-length SpoVD(DTP)) restored
233 normal sporulation (Fig. 3B), the PASTA domain was dispensable as observed previously in
234 *B. subtilis* (Bukowska-Faniband and Hederstedt, 2015). This observation was supported by
235 TEM examination, with morphologically normal spores only observed when the full-length or
236 SpoVD(DT) proteins were expressed (not shown).

237

238 *B. subtilis* SpoVD, and the wider family of class B PBPs, share a conserved active site
239 consisting of 3 non-contiguous motifs that are brought into close proximity in the folded
240 enzyme, SxxK, SxN and KTG (Sauvage et al., 2008). The first of these motifs contains the
241 essential serine nucleophile. SpoVD_{Cd} has all three motifs, with Ser311 as the predicted
242 nucleophile. SpoVD S311A supplied *in trans* was also incapable of complementing the
243 sporulation defect observed in a *spoVD* deletion mutant (Fig. 3B), confirming a role for this
244 residue in cortex synthesis.

245

246 **Subcellular localisation of SpoVD**

247 To visualise the cellular localisation of SpoVD, we fused the coding sequence for SNAP to the
248 5' end of the *spoVD* gene and transferred this to the *C. difficile* genome in the native locus and
249 under the control of the native promoter. SNAP was then labelled with the fluorescent reagent
250 TMR-Start, while newly synthesised peptidoglycan was labelled with the fluorescent D-amino
251 acid HADA (Kuru et al., 2015). Using Airyscan confocal microscopy we observed weak
252 punctate fluorescence around the periphery of the cell, localizing to the asymmetric division
253 septum once the cell had committed to sporulation (Fig. 4A). Fluorescence then tracked the

254 asymmetric membrane through engulfment (Fig. 4B and C), eventually surrounding the
255 prespore (Fig. 4D). Localization of SNAP-SpoVD clearly preceded significant cortex synthesis
256 as we visualised localisation around the spore without concomitant HADA accumulation (Fig.
257 4D). Following further spore maturation (Fig. 4E), accumulation of new HADA-labelled
258 peptidoglycan co-localized with SNAP-SpoVD.

259

260 **SpoVD is required for full resistance to cephalosporins**

261 A comparison of the peptidoglycan composition of wild type and $\Delta spoVD$ cells identified no
262 obvious differences (not shown), suggesting that SpoVD is an exclusive cortex PBP. However,
263 given the extensive complement of PBPs produced by *C. difficile* it is possible that a role in
264 vegetative cell peptidoglycan synthesis could be masked. To determine if SpoVD did
265 contribute to peptidoglycan synthesis more broadly we examined the susceptibility to two PBP-
266 targeting antibiotics, the second- and third-generation cephalosporins cefoxitin and
267 ceftazidime, and the functionally unrelated antibiotic ciprofloxacin. Unsurprisingly deletion of
268 *spoVD* had no effect on ciprofloxacin resistance (Table 3). This mutation did however increase
269 susceptibility to cefoxitin and ceftazidime, decreasing the MIC 4-fold for each, with full
270 resistance restore upon complementation (R20291 $\Delta spoVD$ *pyrE::spoVD*). To identify which
271 SpoVD domains were required for this resistance phenotype we complemented the $\Delta spoVD$
272 mutant with the same panel of SpoVD truncations described above (Table 3). Interestingly,
273 mutant SpoVDs that lacked either the PBP Dimerization (SpoVD(TP)) or the PASTA domains
274 (SpoVD(DT)) were still fully competent for restoring normal cephalosporin resistance, while
275 that lacking the Transpeptidase domain (SpoVD(DP)) displayed the same aberrant sensitivity
276 as the $\Delta spoVD$ mutant. This strongly suggests that only the Transpeptidase domain is required
277 for full cephalosporin resistance. To test if the Transpeptidase alone was sufficient for
278 resistance, we then constructed a truncation consisting of this domain alone. However, this
279 construct did not restore resistance to wild type levels. A full-length SpoVD with a single
280 amino acid substitution, replacing the putative nucleophilic serine with alanine
281 (SpoVD(S311A)), also failed to restore resistance, demonstrating that enzymatic activity is
282 required for the observed cephalosporin resistance.

283

284 Discussion

285 *C. difficile* is the most common cause of hospital acquired infection in the USA and Europe
286 (Magill et al., 2014; Aguado et al., 2015). The formation of a robust spore form is crucial for
287 transmission of infection between patients and for persistence and relapse following treatment
288 (Deakin et al., 2012). However, despite their importance in *C. difficile* pathogenesis, we still
289 know surprisingly little about the underlying molecular mechanisms of sporulation and
290 germination, in part due to a lack of effective genetic tools until recently (Shen, 2019). Much
291 can be learned from the parallels with the well-studied but distantly related species *B. subtilis*,
292 however there are significant differences in the sporulation pathways between the *Bacillales*
293 and *Clostridiales* and even homologous proteins can play subtly different roles (Paredes et al.,
294 2005; Underwood et al., 2009; Fimlaid et al., 2013). Here we have identified and characterised
295 a *C. difficile* homologue of the *B. subtilis* spore cortex PBP SpoVD. We have confirmed that
296 this protein is required for sporulation in *C. difficile* and also identified a surprising role in
297 resistance to cephalosporin antibiotics.

298

299 Bioinformatic analysis of the *C. difficile* genome identified 10 genes encoding proteins with
300 significant homology to characterised *B. subtilis* PBPs. In a previous transposon mutagenesis
301 screen we determined that only two of these are essential for growth *in vitro*, but five were
302 required for formation of heat-resistant spores (Dembek et al., 2015). One of these
303 (R20291_2544) encodes a protein sharing 27.9% amino acid identity with *B. subtilis* SpoVD.
304 Despite this relatively weak homology, the two proteins share a similar overall domain
305 organisation and are encoded in a similar genomic context. To determine if this protein played
306 a role in *C. difficile* sporulation we constructed a clean deletion mutant that we found to be
307 incapable of producing viable spores. Microscopic examination of this mutant allowed us to
308 visualise fully engulfed prespores but these structures lacked any obvious cortex. This
309 sporulation defect was fully complemented by integration of *spoVD* (and the upstream
310 R20291_2545 and native promoter) in a distal chromosomal locus. These observations clearly
311 demonstrated that SpoVD plays a crucial role in *C. difficile* sporulation and is required for the
312 synthesis of cortex peptidoglycan. We then demonstrated that the sporulation defect in a *spoVD*
313 mutant could be complemented by expression *in trans* of a mutant SpoVD lacking the C
314 terminal PASTA domain but that mutation of the PBP dimerization or transpeptidase domains
315 resulted in a non-functional SpoVD. This is in full agreement with previous *B. subtilis* studies
316 that showed that the PASTA domain was dispensable for cortex synthesis (Bukowska-
317 Faniband and Hederstedt, 2015). By comparison with the *B. subtilis* sequence we were also

318 able to putatively identify the active site nucleophile serine as S311 and confirmed this role by
319 mutation to alanine, resulting in a non-functional SpoVD.

320

321 It has been shown previously that *B subtilis* SpoVD localises to the asymmetric septum upon
322 initiation of sporulation and ultimately to the developing spore following engulfment (Sidarta
323 et al., 2018). To visualise this process in *C. difficile* we generated a strain expressing SNAP-
324 SpoVD under the control of the native promoter. Super-resolution fluorescence microscopy
325 imaging of this strain showed clear localisation of SNAP-SpoVD to the asymmetric septum
326 and to the developing spore. Intriguingly we also observed weak punctate fluorescence staining
327 around the periphery of the mother cell. This could be indicative of mislocalisation as a result
328 of the N terminal SNAP fusion or could suggest a broader role for SpoVD in vegetative cell
329 peptidoglycan synthesis. To test this latter possibility, we examined the peptidoglycan
330 composition of wild type and *spoVD* mutant cells but observed no obvious differences. Given
331 the enormous potential for redundancy with 10 encoded PBPs it is possible that small
332 differences could be missed in this analysis. To examine more subtle effects, we analysed
333 resistance to two PBP-targeting cephalosporin antibiotics, cefoxitin and ceftazidime.
334 Surprisingly the *spoVD* mutant displayed a 4-fold reduction in MIC to both antibiotics.
335 Although small, this difference in MIC was reproducible and complemented perfectly when
336 *spoVD* was added back. This unexpected observation strongly suggests that SpoVD is active
337 in vegetative cells and is not spore-specific as has been suggested for *B. subtilis*.

338

339 Sporulation of *C. difficile* represents one of the most pressing clinical challenges in tackling
340 recurrent disease in individual patients as well as preventing outbreaks in nosocomial settings.
341 However, this cell differentiation pathway also represents a promising target for the
342 development of *C. difficile*-specific therapeutics. In order to exploit this potential we must first
343 develop a deeper understanding of both the complex regulatory processes that underpin
344 sporulation as well as the function of the effector proteins that direct differentiation. Here we
345 have identified and characterised a PBP that is absolutely required for production of viable
346 spores and that we believe is a promising target for future therapeutics aimed at preventing
347 recurrent disease and transmission.

348

349 **Acknowledgements**

350 We would like to thank Darren Robinson and Christa Walther (The Wolfson Light Microscopy
351 Facility, University of Sheffield) for their light microscopy support and training, Stephane
352 Mesnage (University of Sheffield) for assistance with peptidoglycan analysis, Chris Hill
353 (Electron Microscopy Unit, University of Sheffield) for thin sectioning and transmission
354 electron microscopy, Nigel Minton (University of Nottingham) for supplying plasmids for
355 homologous recombination, Adriano Henriques for supplying pFT46, and Simon Jones and
356 Shuwen Ma (University of Sheffield) for synthesis of HADA.

357

358 **Funding**

359 This work was supported by a PhD studentship from the Higher Committee for Education and
360 Development in Iraq for Y.A.A. and by the Medical Research Council (P.O., grant number
361 MR/N000900/1) and the Wellcome Trust (J.A.K., grant number 204877/Z/16/Z). The funders
362 had no role in study design, data collection and interpretation, or the decision to submit the
363 work for publication.

364

365 **Author contributions**

366 Y.A.A. and R.P.F. designed and coordinated the study. Y.A.A., P.O. and J.A.K. performed the
367 experiments. R.P.F. wrote the paper with input from all co-authors.

368

369 **Conflicts of interest**

370 The authors declare that the research was conducted in the absence of any commercial or
371 financial relationships that could be construed as a potential conflict of interest.

372

373 **References**

- 374 Aguado, J.M., Anttila, V.J., Galperine, T., Goldenberg, S.D., Gwynn, S., Jenkins, D., et al.
375 (2015). Highlighting clinical needs in *Clostridium difficile* infection: the views of
376 European healthcare professionals at the front line. *J Hosp Infect* 90(2), 117-125. doi:
377 10.1016/j.jhin.2015.03.001.
- 378 Bukowska-Faniband, E., and Hederstedt, L. (2015). The PASTA domain of penicillin-binding
379 protein SpoVD is dispensable for endospore cortex peptidoglycan assembly in *Bacillus*
380 *subtilis*. *Microbiology* 161(Pt 2), 330-340. doi: 10.1099/mic.0.000011.
- 381 Cartman, S.T., Kelly, M.L., Heeg, D., Heap, J.T., and Minton, N.P. (2012). Precise
382 manipulation of the *Clostridium difficile* chromosome reveals a lack of association
383 between the tcdC genotype and toxin production. *Appl Environ Microbiol* 78(13),
384 4683-4690. doi: 10.1128/AEM.00249-12.
- 385 Clinical and Laboratory Standards Institute (2012). "Methods for antimicrobial susceptibility
386 testing of anaerobic bacteria; approved standard". 8th ed. CLSI document M11-A8. ed.
387 (Wayne, PA: Clinical and Laboratory Standards Institute).
- 388 Daniel, R.A., Drake, S., Buchanan, C.E., Scholle, R., and Errington, J. (1994). The *Bacillus*
389 *subtilis* *spoVD* gene encodes a mother-cell-specific penicillin-binding protein required
390 for spore morphogenesis. *J Mol Biol* 235(1), 209-220. doi: 10.1016/s0022-
391 2836(05)80027-0.
- 392 Deakin, L.J., Clare, S., Fagan, R.P., Dawson, L.F., Pickard, D.J., West, M.R., et al. (2012). The
393 *Clostridium difficile* *spo0A* gene is a persistence and transmission factor. *Infection and*
394 *Immunity* 80(8), 2704-2711. doi: 10.1128/IAI.00147-12.
- 395 Dembek, M., Barquist, L., Boinett, C.J., Cain, A.K., Mayho, M., Lawley, T.D., et al. (2015).
396 High-throughput analysis of gene essentiality and sporulation in *Clostridium difficile*.
397 *MBio* 6(2), e02383. doi: 10.1128/mBio.02383-14.
- 398 Dupuy, B., and Sonenshein, A.L. (1998). Regulated transcription of *Clostridium difficile* toxin
399 genes. *Mol Microbiol* 27(1), 107-120. doi: [https://doi.org/10.1046/j.1365-](https://doi.org/10.1046/j.1365-2958.1998.00663.x)
400 2958.1998.00663.x.
- 401 Dyer, C., Hutt, L.P., Burky, R., and Joshi, L.T. (2019). Biocide resistance and transmission of
402 *Clostridium difficile* spores spiked onto clinical surfaces from an American healthcare
403 facility. *Appl Environ Microbiol*. doi: 10.1128/AEM.01090-19.
- 404 El-Gebali, S., Mistry, J., Bateman, A., Eddy, S.R., Luciani, A., Potter, S.C., et al. (2019). The
405 Pfam protein families database in 2019. *Nucleic Acids Res* 47(D1), D427-D432. doi:
406 10.1093/nar/gky995.

- 407 Fagan, R.P., and Fairweather, N.F. (2011). *Clostridium difficile* has two parallel and essential
408 Sec secretion systems. *Journal of Biological Chemistry* 286(31), 27483-27493. doi:
409 10.1074/jbc.M111.263889.
- 410 Fay, A., Meyer, P., and Dworkin, J. (2010). Interactions between late-acting proteins required
411 for peptidoglycan synthesis during sporulation. *J Mol Biol* 399(4), 547-561. doi:
412 10.1016/j.jmb.2010.04.036.
- 413 Fimlaid, K.A., Bond, J.P., Schutz, K.C., Putnam, E.E., Leung, J.M., Lawley, T.D., et al. (2013).
414 Global analysis of the sporulation pathway of *Clostridium difficile*. *PLoS Genet* 9(8),
415 e1003660. doi: 10.1371/journal.pgen.1003660.
- 416 Gilmore, M.E., Bandyopadhyay, D., Dean, A.M., Linnstaedt, S.D., and Popham, D.L. (2004).
417 Production of muramic delta-lactam in *Bacillus subtilis* spore peptidoglycan. *J*
418 *Bacteriol* 186(1), 80-89. doi: 10.1128/jb.186.1.80-89.2004.
- 419 He, M., Miyajima, F., Roberts, P., Ellison, L., Pickard, D.J., Martin, M.J., et al. (2013).
420 Emergence and global spread of epidemic healthcare-associated *Clostridium difficile*.
421 *Nat Genet* 45(1), 109-113. doi: 10.1038/ng.2478.
- 422 Kirk, J.A., and Fagan, R.P. (2016). Heat shock increases conjugation efficiency in *Clostridium*
423 *difficile*. *Anaerobe* 42, 1-5. doi: 10.1016/j.anaerobe.2016.06.009.
- 424 Kuru, E., Tekkam, S., Hall, E., Brun, Y.V., and Van Nieuwenhze, M.S. (2015). Synthesis of
425 fluorescent D-amino acids and their use for probing peptidoglycan synthesis and
426 bacterial growth in situ. *Nat Protoc* 10(1), 33-52. doi: 10.1038/nprot.2014.197.
- 427 Lessa, F.C., Mu, Y., Bamberg, W.M., Beldavs, Z.G., Dumyati, G.K., Dunn, J.R., et al. (2015).
428 Burden of *Clostridium difficile* infection in the United States. *N Engl J Med* 372(9),
429 825-834. doi: 10.1056/NEJMoa1408913.
- 430 Magill, S.S., Edwards, J.R., Bamberg, W., Beldavs, Z.G., Dumyati, G., Kainer, M.A., et al.
431 (2014). Multistate point-prevalence survey of health care-associated infections. *N Engl*
432 *J Med* 370(13), 1198-1208. doi: 10.1056/NEJMoa1306801.
- 433 Meador-Parton, J., and Popham, D.L. (2000). Structural analysis of *Bacillus subtilis* spore
434 peptidoglycan during sporulation. *J Bacteriol* 182(16), 4491-4499. doi:
435 10.1128/jb.182.16.4491-4499.2000.
- 436 Ng, Y.K., Ehsaan, M., Philip, S., Collery, M.M., Janoir, C., Collignon, A., et al. (2013).
437 Expanding the repertoire of gene tools for precise manipulation of the *Clostridium*
438 *difficile* genome: allelic exchange using *pyrE* alleles. *PLoS One* 8(2), e56051. doi:
439 10.1371/journal.pone.0056051.

- 440 Paredes, C.J., Alsaker, K.V., and Papoutsakis, E.T. (2005). A comparative genomic view of
441 clostridial sporulation and physiology. *Nat Rev Microbiol* 3(12), 969-978. doi:
442 10.1038/nrmicro1288.
- 443 Paredes-Sabja, D., Shen, A., and Sorg, J.A. (2014). *Clostridium difficile* spore biology:
444 sporulation, germination, and spore structural proteins. *Trends Microbiol* 22(7), 406-
445 416. doi: 10.1016/j.tim.2014.04.003.
- 446 Peltier, J., Courtin, P., El Meouche, I., Lemeec, L., Chapot-Chartier, M.P., and Pons, J.L. (2011).
447 *Clostridium difficile* has an original peptidoglycan structure with a high level of N-
448 acetylglucosamine deacetylation and mainly 3-3 cross-links. *J Biol Chem* 286(33),
449 29053-29062. doi: 10.1074/jbc.M111.259150.
- 450 Pereira, F.C., Saujet, L., Tome, A.R., Serrano, M., Monot, M., Couture-Tosi, E., et al. (2013).
451 The spore differentiation pathway in the enteric pathogen *Clostridium difficile*. *PLoS*
452 *Genet* 9(10), e1003782. doi: 10.1371/journal.pgen.1003782.
- 453 Purdy, D., O'Keeffe, T.A., Elmore, M., Herbert, M., McLeod, A., Bokori-Brown, M., et al.
454 (2002). Conjugative transfer of clostridial shuttle vectors from *Escherichia coli* to
455 *Clostridium difficile* through circumvention of the restriction barrier. *Mol Microbiol*
456 46(2), 439-452. doi: <https://doi.org/10.1046/j.1365-2958.2002.03134.x>.
- 457 Rupnik, M., Wilcox, M.H., and Gerding, D.N. (2009). *Clostridium difficile* infection: new
458 developments in epidemiology and pathogenesis. *Nat Rev Microbiol* 7(7), 526-536. doi:
459 <https://doi.org/10.1038/nrmicro2164>.
- 460 Sauvage, E., Kerff, F., Terrak, M., Ayala, J.A., and Charlier, P. (2008). The penicillin-binding
461 proteins: structure and role in peptidoglycan biosynthesis. *FEMS Microbiol Rev* 32(2),
462 234-258. doi: 10.1111/j.1574-6976.2008.00105.x.
- 463 Schindelin, J., Arganda-Carreras, I., Frise, E., Kaynig, V., Longair, M., Pietzsch, T., et al.
464 (2012). Fiji: an open-source platform for biological-image analysis. *Nat Methods* 9(7),
465 676-682. doi: 10.1038/nmeth.2019.
- 466 Shen, A. (2019). Expanding the *Clostridioides difficile* genetics toolbox. *J Bacteriol.* doi:
467 10.1128/JB.00089-19.
- 468 Sidarta, M., Li, D., Hederstedt, L., and Bukowska-Faniband, E. (2018). Forespore Targeting
469 of SpoVD in *Bacillus subtilis* Is Mediated by the N-Terminal Part of the Protein. *J*
470 *Bacteriol* 200(13). doi: 10.1128/JB.00163-18.
- 471 Smits, W.K., Lyras, D., Lacy, D.B., Wilcox, M.H., and Kuijper, E.J. (2016). *Clostridium*
472 *difficile* infection. *Nat Rev Dis Primers* 2, 16020. doi: 10.1038/nrdp.2016.20.

- 473 Stabler, R.A., He, M., Dawson, L., Martin, M., Valiente, E., Corton, C., et al. (2009).
474 Comparative genome and phenotypic analysis of *Clostridium difficile* 027 strains
475 provides insight into the evolution of a hypervirulent bacterium. *Genome Biol* 10(9),
476 R102. doi: 10.1186/gb-2009-10-9-r102.
- 477 Underwood, S., Guan, S., Vijayasubhash, V., Baines, S.D., Graham, L., Lewis, R.J., et al.
478 (2009). Characterization of the sporulation initiation pathway of *Clostridium difficile*
479 and its role in toxin production. *J Bacteriol* 191(23), 7296-7305. doi:
480 10.1128/JB.00882-09.
- 481 Zhu, D., Sorg, J.A., and Sun, X. (2018). *Clostridioides difficile* Biology: Sporulation,
482 Germination, and Corresponding Therapies for *C. difficile* Infection. *Front Cell Infect*
483 *Microbiol* 8, 29. doi: 10.3389/fcimb.2018.00029.
- 484
- 485

486 **Tables**

487

488 **Table 1:** Strains, plasmids and oligonucleotides used in this study

Strain	Characteristics	Source
R20291	<i>C. difficile</i> ribotype 027 strain isolated during an outbreak at Stoke Mandeville hospital, UK in 2006.	(Stabler et al., 2009)
R20291 Δ <i>pyrE</i>	An R20291 <i>pyrE</i> deletion mutant.	(Ng et al., 2013)
R20291 Δ <i>spoVD</i>	R20291 with the entire <i>spoVD</i> gene, except the first and last three codons, deleted.	This study
R20291 Δ <i>spoVD pyrE::spoVD</i>	R20291 Δ <i>spoVD</i> complemented by simultaneous restoration of the wild type <i>pyrE</i> gene and insertion of <i>spoVD</i> under the native promoter between <i>pyrE</i> and the downstream R20291_0189.	This study
R20291 <i>snap-spoVD</i>	R20291 with the native <i>spoVD</i> locus modified by homologous recombination to add the coding sequence of SNAP to the 5' end of <i>spoVD</i> .	This study
CA434	<i>E. coli</i> conjugative donor. HB101 carrying R702.	(Purdy et al., 2002)
NEB5 α	<i>fhuA2</i> Δ (<i>argF-lacZ</i>)U169 <i>phoA glnV44</i> Φ 80 Δ (<i>lacZ</i>)M15 <i>gyrA96 recA1 relA1 endA1 thi-1 hsdR17</i> .	New England Biolabs
Plasmid	Characteristics	Source
pMTL960	<i>E. coli-C. difficile</i> shuttle vector.	Nigel Minton
pRPF150	P _{<i>cwp2</i>} - <i>Strep</i> -tag II- <i>secA2</i> cassette cloned between KpnI and BamHI sites in pMTL960.	(Fagan and Fairweather, 2011)
pJAK012	pRPF150 modified to introduce an XhoI site between <i>Strep</i> -tag II encoding sequence and the <i>secA2</i> gene.	This study

pJAK032	Strep Tag II coding sequence in pJAK012 replaced with a codon-optimized <i>clip</i> gene.	This study
pFT46	Plasmid containing a <i>C. difficile</i> codon-optimized copy of the <i>snap</i> gene under the control of a tetracycline inducible promoter.	(Pereira et al., 2013)
pMTL-YN4	Allele exchange vector for <i>pyrE</i> -based selection.	(Ng et al., 2013)
pMTL-YN2C	<i>pyrE</i> restoration vector allowing simultaneous insertion of cargo DNA between <i>pyrE</i> and R20291_0189.	(Ng et al., 2013)
pMTL-SC7215	Allele exchange vector for <i>codA</i> -based selection.	(Cartman et al., 2012)
pYAA024	<i>spoVD</i> deletion: 1,200 bp homology arms representing the sequence upstream and downstream of R20291_2544 (<i>spoVD</i>) cloned into pMTL-YN4. Designed to delete all but the first and last 9 bp of <i>spoVD</i> .	This study
pYAA027	SpoVD complementation: <i>spoVD</i> and its native promoter cloned into pMTLYN2C.	This study
pYAA031	Constitutive CLIP-SpoVD: <i>spoVD</i> cloned between XhoI and BamHI sites in pJAK032.	This study
pYAA047	SNAP-SpoVD: 1,200 bp upstream of <i>spoVD</i> was fused to the coding sequence of SNAP and the first 1,200 bp of <i>spoVD</i> and the subsequent recombination cassette cloned into pMTL-SC7215.	This study
pYAA048	SpoVD(TP): pYAA031 modified by deletion of the sequence encoding the SpoVD PBP dimerization domain.	This study
pYAA049	SpoVD(DT): pYAA031 modified by deletion of the sequence encoding the SpoVD PASTA domain.	This study

pYAA050	SpoVD(DP): pYAA031 modified by deletion of the sequence encoding the SpoVD transpeptidase domain.	This study
pYAA051	SpoVD(T): pYAA031 modified by deletion of the sequence encoding the SpoVD PBP dimerization and PASTA domains.	This study
pYAA052	His-SpoVD: <i>spoVD</i> cloned into pET-28a between NcoI and XhoI sites.	This study

Oligonucleotide	Sequence	Use
NF1957	<u>GAGTCAGTTATAGATTCGATACTTGA</u> C	To introduce an XhoI site into pRPF150 by inverse PCR with NF1958
NF1958	<u>GAGTTTTTCAAATTGTGGATGACTCC</u> AC	To introduce an XhoI site into pRPF150 by inverse PCR with NF1957
RF20	AAACTCCTTTTTGATAATCTCATGAC C	To linearize pMTL-SC7215 with RF311
RF139*	GTCAG <u>GAGCTCGTTCTTTATTTAGATTA</u> AATAAAGTCAATG	To clone <i>spoVD</i> into pMTL-YN4 with RF187
RF187*	GTCAG <u>GATCCCTTAGGAATCAGAGAG</u> TAGATAG	To clone <i>spoVD</i> into pMTL-YN4 with RF139
RF226	GATC <u>GAGCTCGGAGGA</u> ACTACTATGG ATAAAGATTGTGAAATGAAAAG	To add a 5' SacI site onto a codon optimised <i>clip</i> gene fragment
RF227	GATC <u>CTCGAGAGCAGCTGCTCCTAAT</u> CCTGGTTTTCCCTAATC	To add 3xAla codons and a 3' XhoI site onto a codon optimised <i>clip</i> gene fragment
RF311	TAGGGTAACAAAAAACACCG	To linearize pMTL-SC7215 with RF20

RF323*	GTCAGGATCCGTTTATGGGTATATGT TAATTATCTGTTAC	To clone R20291_2545 and <i>spoVD</i> into pMTL- YN2C with RF324
RF324*	GTCAGAGCTCCTTAGGAATCAGAGAG TAGATAG	To clone R20291_2545 and <i>spoVD</i> into pMTL- YN2C with RF323
RF374*	GATCCTCGAGAGAAAAGTAAAGAGG ATAAGTAAGAAAAGG	To clone <i>spoVD</i> into pJAK032 with RF375
RF375*	GTCAGGATCCCTTAGTTTTCAAATAT AGGGTTATACTTGAG	To clone <i>spoVD</i> into pJAK032 with RF374
RF461	CTCAAATCTATTCCCCCTAGTTATCC	To amplify <i>spoVD</i> promoter probe with RF462 for Southern blotting
RF462	GAATCTATGTGGTTATTCAAAAATCT CG	To amplify <i>spoVD</i> promoter probe with RF462 for Southern blotting
RF528	aaatacgggtgtttttgttacctaagtttAAGCTAGAA TAGATGGACC	To amplify 1,200 bp homology arm upstream of <i>spoVD</i>
RF529	acaatctttatccatATCTATTCCCCCTAGTTA TCC	To amplify 1,200 bp homology arm upstream of <i>spoVD</i>
RF530	ctagggggaatagatATGGATAAAGATTGTG AAATGAAGAGAACCAC	To amplify <i>snap</i>
RF531	cctctttactttctAGCAGCTGCCCAAGTCC	To amplify <i>snap</i>
RF532	cttgggcagctgctAGAAAAGTAAAGAGGA TAAGTAAGAAAAG	To amplify first 1,200 bp of <i>spoVD</i>
RF533	tttgatcatgagattatcaaaaaggagttTAAATCTAT ACCTGTCTTATCCATAAG	To amplify first 1,200 bp of <i>spoVD</i>
RF582	TATATCTCTTGTGTTGTTCTAGTGC TTTTG	To delete the coding sequence of the <i>SpoVD</i>

		PBP Dimerization domain with RF583
RF583	GCAAAAAAGGTTACTGCAATAGCTAT G	To delete the coding sequence of the SpoVD PBP Dimerization domain with RF582
RF584	GGTTAACTCCCAAATATTTTAAAGA GTCATTC	To delete the coding sequence of the SpoVD PASTA domain with RF585
RF585	TAAGGATCCACTAGTAACGGCC	To delete the coding sequence of the SpoVD PASTA domain with RF584
RF586	AGTATATAAAGAAGAAGAAAAAGCT GAGTATG	To delete the coding sequence of the SpoVD Transpeptidase domain with RF587
RF587	ATTATTTAACTCATAAGCTTTCTGTAC TGC	To delete the coding sequence of the SpoVD Transpeptidase domain with RF586

489 *Restriction endonuclease sites are underlined

490

491 **Table 2:** Putative *C. difficile* PBPs.

<i>C. difficile</i> R20291 gene designation	Best <i>B. subtilis</i> strain 168 hit	Amino acid identity	Essential <i>in vitro</i> ?
0712	PonA	27.3%	Yes
2544	SpoVD	40.1%	No but required for sporulation
1067	SpoVD	27.9% (PbpB 26.6%)	No but required for sporulation

1131	DacF	43.8%	No but required for sporulation
1318	PbpX	21.3% (PbpE 20.4%)	No
2048	DacF	31.5%	No but required for sporulation
0441	DacF	30.3%	No
0985	PbpA	21.2%	Yes
3056	PbpX	20.1%	No but required for sporulation
2390	DacB	27.5%	No

492

493 **Table 3:** Antibiotic MICs ($\mu\text{g/ml}$).

Strain	Cefoxitin	Ceftazidime	Ciprofloxacin
R20291	128	256	512
R20291 Δ <i>spoVD</i>	32	64	512
R20291 Δ <i>spoVD pyrE::spoVD</i>	128	256	512
R20291 Δ <i>spoVD</i> +SpoVD(DTP)	128	256	n.d.
R20291 Δ <i>spoVD</i> +SpoVD(TP)	128	256	n.d.
R20291 Δ <i>spoVD</i> +SpoVD(DT)	128	256	n.d.
R20291 Δ <i>spoVD</i> +SpoVD(DP)	32	64	n.d.
R20291 Δ <i>spoVD</i> +SpoVD(T)	32	64	n.d.
R20291 Δ <i>spoVD</i> +SpoVD(S311A)	32	64	n.d.

494

495

496 **Figure legends**

497

498 **Figure 1:** Sporulation requires SpoVD. **A.** Genomic organisation of the native *spoVD* locus
499 (WT), following deletion of the *spoVD* gene (Δ) and following complementation by insertion
500 of R20291_2545 and *spoVD* between the *pyrE* and R20291_0189 genes (Comp). The locations
501 of XmnI (X) and BsrGI (B) sites are indicated, as is the annealing site of the Southern blot
502 probe. The length of the diagnostic restriction product containing the probe sequence is also
503 shown below each locus diagram. **B.** Southern blot analysis of a *spoVD* mutant
504 (R20291 Δ *spoVD*), the wild type parental strain (R20291) and complemented strain
505 (R20291 Δ *spoVD pyrE::spoVD*). A DNA ladder is shown on the left hand side. The predicted
506 fragment sizes and annealing site of the probe are shown in panel A. **C.-E.** Sporulation
507 efficiencies of the wild type (**C.**), *spoVD* mutant (**D.**) and complemented strains (**E.**). Stationary
508 phase cultures were incubated anaerobically for 5 days with samples taken daily to enumerate
509 total colony forming units (CFUs) and spores, following heat treatment to kill vegetative cells.
510 Experiments were performed in duplicate on biological triplicates with mean and standard
511 deviation shown. The dotted horizontal line indicates the limit of detection of the experiment.

512

513 **Figure 2:** Microscopic analysis of sporulation. Phase contrast light microscopy (**A.**) and
514 negative stained TEM (**B.**) of the wild type parental strain (R20291), *spoVD* mutant
515 (R20291 Δ *spoVD*) and complemented strain (R20291 Δ *spoVD pyrE::spoVD*). **A.** Cultures were
516 imaged at day 5 of the sporulation assays shown in Figure 1. Spores are visible as ovoid phase
517 bright objects i, while vegetative cells are phase dark bacilli. **B.** TEM imaging of developing
518 spores clearly shows normal spore development in R20291 and R20291 Δ *spoVD pyrE::spoVD*;
519 the densely stained core surrounded by a thick, largely unstained cortex layer. Cultures of
520 R20291 Δ *spoVD* contained no morphologically normal developing spores, although fully
521 engulfed prespores without a cortex (example shown) were common.

522

523 **Figure 3:** The contribution of SpoVD domains to sporulation. **A.** The domain organisation of
524 SpoVD showing Pfam predictions (El-Gebali et al., 2019). **B.** Sporulation efficiency of
525 R20291, R20291 Δ *spoVD* and R20291 Δ *spoVD* complemented *in trans* using a plasmid
526 expressing a series of mutant SpoVDs under the control of a constitutive promoter: full-length
527 SpoVD (DTP); SpoVD lacking the PBP dimerization domain (TP), PASTA domain (DT),
528 transpeptidase domain (DP) or both PBP dimerization and PASTA domains (T); SpoVD

529 lacking the active site nucleophile serine (S311A). Shown is the sporulation efficiency after 5
530 days in broth culture, expressed as number of spores as a percentage of total viable CFUs.
531 Experiments were conducted in duplicate on biological triplicates and mean and standard
532 deviations are shown.

533

534 **Figure 4:** Subcellular localisation of SpoVD. R20291 *snap-spoVD* was grown for 24 h in TY
535 broth containing the fluorescent D-amino acid HADA (500 nM) to label *de novo* synthesised
536 peptidoglycan. The bacteria were then further stained with SNAP-Cell TMR-Star (250 nM) to
537 label SNAP-SpoVD, fixed, mounted in SlowFade Diamond mountant and imaged using a Zeiss
538 AiryScan confocal microscope. Shown are representative cells demonstrating the sequential
539 stages of sporulation: **A.** asymmetric septum placement, **B.**, **C.** and **D.** early, mid and complete
540 prespore engulfment respectively, **E.** spore maturation.

541

542

Figure 1

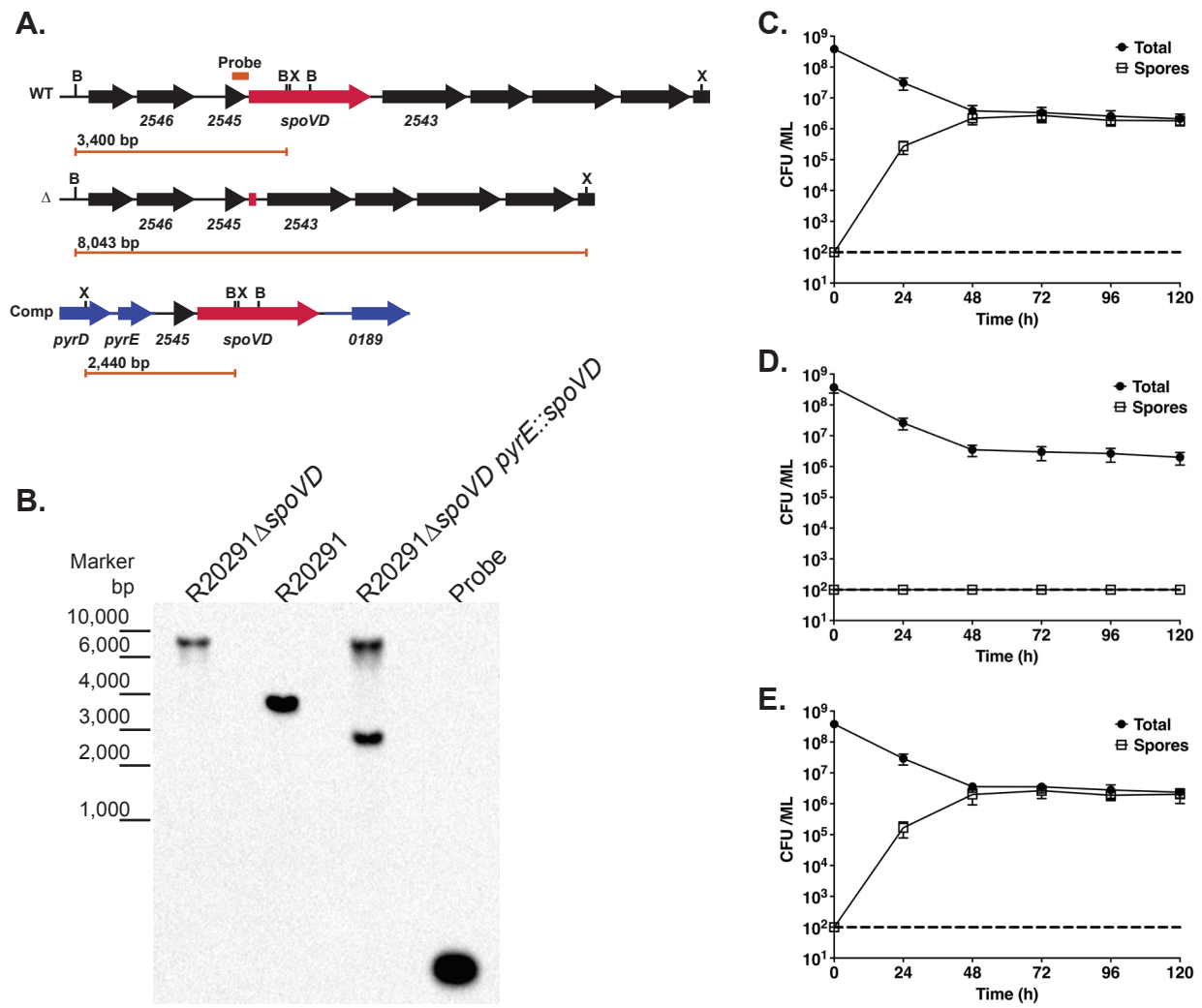


Figure 2

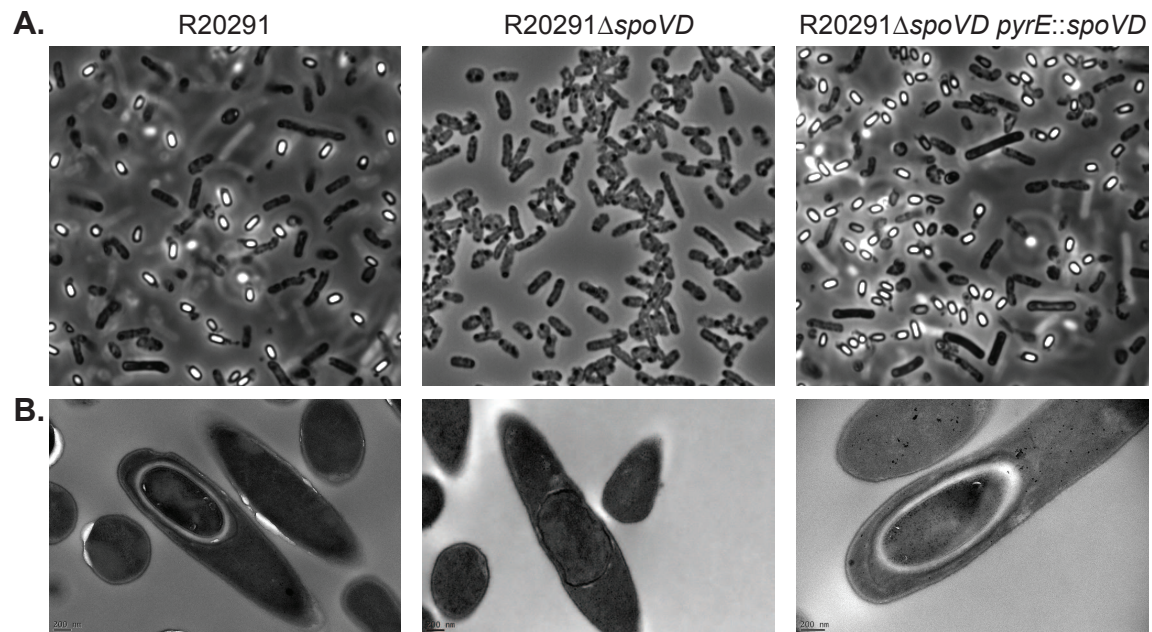


Figure 3

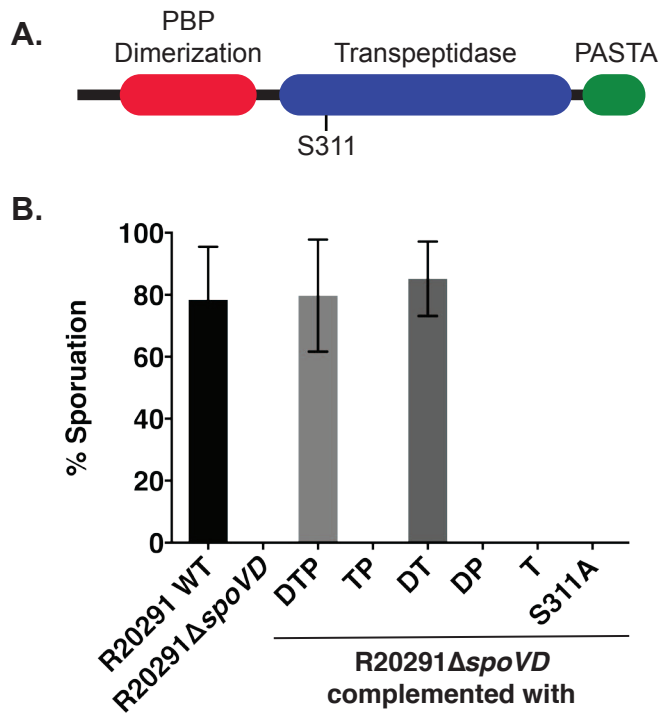


Figure 4

